Multi-photon upconversion luminescence of Er^{3+}-doped Y_2O_3 nanocrystals

Yunxiang Wang (王云祥)[1], Yunfeng Bai (白云峰)[2], and Yinglin Song (宋瑛林)[1*]

[1] *School of Physical Science and Technology, Soochow University, Soochow 215006, China*

[2] *Department of Physics, Harbin Institute of Technology, Harbin 150001, China*

[*] *E-mail: ylsong@hit.edu.cn*

Received September 12, 2008

Visible upconversion emission intensities are investigated in Er^{3+}-doped Y_2O_3 nanocrystals. We also find that the upconversion intensity varies nonlinearly with the excitation power with a threshold of 110 mW, which indicates that the green and red emissions would be photon avalanche upconversion when the excitation power exceeds the threshold.

OCIS codes: 190.7220, 160.4236, 250.5230, 160.5690.

doi: 10.3788/COL20090706.0524.

Some oxides doped with rare earth (RE) ions are important phosphors and thus the corresponding nanocrystals (NCs) have attracted considerable attention[1,2]. In the past decade, Er^{3+}-doped materials have attracted great attention[2−5]. Photoluminescence (PL) and upconversion photoluminescence (Up-PL) in Er^{3+}-doped ZnO/Y_2O_3 NC have been investigated[6−9]. Y_2O_3 is an attractive host material for laser applications due to its high melting point (2380 °C) and high thermal conductivity[10]. Y_2O_3 doped with RE^{3+} phosphors is extensively used in optical display and light-emitting devices. The trend towards nanoscale science has raised interests in preparation of various Y_2O_3 nanostructures[10,11].

In this letter, we report the multiphoton upconversion luminescence of Er^{3+} in the Er^{3+}-doped Y_2O_3 NC. We also study the luminescence mechanism. Under low excitation power, the mechanism can be described as two-photon absorption (TPA). However, it should be a photon avalanche upconversion phenomenon under high excitation power.

We utilized a precursor method to prepare Y_2O_3 NC which was doped with 2-mol% Er^{3+}. We firstly dissolved $Y(NO_3)_3{\cdot}6H_2O$ and $Er(NO_3)_3{\cdot}6H_2O$ with predetermined concentrations in de-ionized water at 80 °C. Citric acid was then added to the solution with the mole ratio of (Y^{3+}+Er^{3+}) to citric acid to be 1:3; ammonium hydroxide serving as a pH adjuster was subsequently added. We churned the resulting solution until it was transformed into a black bulk solid. The solid was dried in air at 150 °C for 2 h, and further calcined in air at 800 °C for 2 h. The final material in powder form was pressed to form smooth and flat disks for spectral studies.

X-ray diffraction (XRD) studies were carried out on the Y_2O_3 NC powder doped with 2-mol% Er^{3+}. Figure 1 shows the XRD patterns. The diffraction peaks coincide with the standard values of the highly crystalline Y_2O_3 crystal (JCPDS No. 41-1105). This indicates that the main structure of Y_2O_3 in the sample is cubic.

A diode laser emitting at 976 nm with the full-width at half-maximum (FWHM) of 2 nm was used to irradiate the sample. The maximum excitation power was about 250 mW. At room temperature, the Up-PL intensity of the sample was collected using a SPEX1000M spectrometer with a spectral resolution of 1 nm.

Figure 2 shows the Up-PL spectra of the Er^{3+}-doped Y_2O_3 specimens at room temperature. The excitation power is 40 mW. There are two distinctive bands associated with the Er^{3+} ions observed in green and red regions. The green emission observed between 520−570 nm arises from the transitions of $^2H_{11/2}$ and $^4S_{3/2}$ excited states

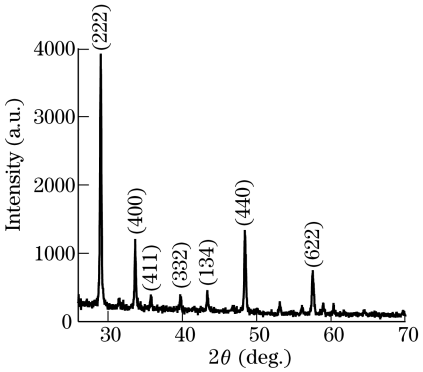

Fig. 1. XRD pattern of Er^{3+}-doped Y_2O_3 NC power containing 2-mol% Er^{3+}.

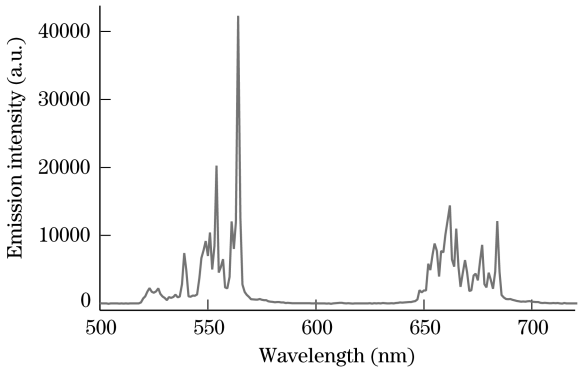

Fig. 2. Up-PL spectra of Er^{3+} in Y_2O_3 NC doped with 2-mol% Er^{3+} in the visible region under excitation with a diode laser emitting at 976-nm wavelength.

to the $^4I_{15/2}$ ground state, and the red spectra observed in the range of 650−690 nm is due to the $^4F_{9/2} \rightarrow {}^4I_{15/2}$ transition.

The excitation power dependences of the green and red emissions of Y_2O_3NC doped with 2-mol% Er^{3+} ions are shown in Fig. 3. It can be seen that both the slopes of red and green emissions are always the same at all excitation power. It is generally accepted that the slope of the luminescence intensity versus pump power in a double-logarithmic plot provides information on the number of pump photons required to excite the emitting levels[12]. So in our experiment, at low excitation power, both the slopes of green and red emissions are about 1.6. Then we know that it should be a two-photon mechanism upconversion. But when the excitation power exceeds 110 mW, both the green and red emissions increase quickly, indicating that both emissions should be generated through multi-photon photon process. It may be a new photon avalanche upconversion when the excitation power exceeds the threshold.

In Fig. 4, it is shown that under low excitation power, an Er^{3+} in the ground state $^4I_{15/2}$ absorbs a photon and transits to the state $^4I_{11/2}$, and then a second 976-nm photon can populate the $^4F_{7/2}$ level of Er^{3+} ion. The Er^{3+} ion can then relax nonradiatively to the $^2H_{11/2}$ and $^4S_{3/2}$ levels, and the $^2H_{11/2} \rightarrow {}^4I_{15/2}$ and $^4S_{3/2} \rightarrow {}^4I_{15/2}$ green emissions occur. Also, the Er^{3+} ion in the $^4I_{11/2}$ state may nonradiatively decay to the $^4I_{13/2}$ state and then populate the state $^4F_{9/2}$via absorbing a 976-nm photon, leading to the $^4F_{9/2} \rightarrow {}^4I_{15/2}$ red emission[13].

It is generally known that the luminescence intensity increases with the increasing excitation power gradually, and the double-logarithmic plot of the luminescence intensity versus pump power is nearly linear. But in our experiment, the luminescence intensity increases greatly when the pump power exceeds 110 mW, so does the slope of the double-logarithmic plot, just as Fig. 3 shows. From the above analysis, it should be a multi-photon upconversion mechanism. However, we think the probability of both red and green emissions are most likely generated through photon avalanche upconversion, because the emission intensity increases quickly and this phenomenon even can be found with naked eyes. To our knowledge, it is the first report of photon avalanche

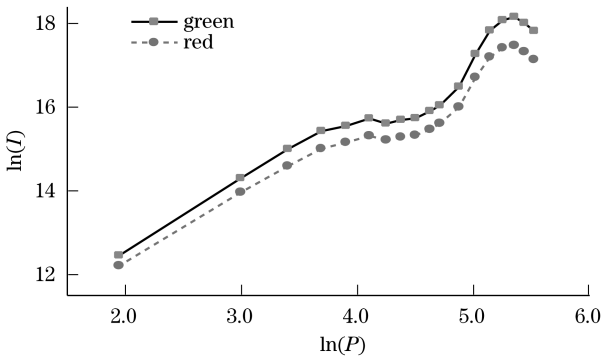

Fig. 3. Pump power dependences of the green and red emissions of Y_2O_3 NC doped with 2-mol% Er^{3+} ions in double-logarithmic representation. I is the luminescence intensity in arbitrary units, P is the pump power in milliwatts.

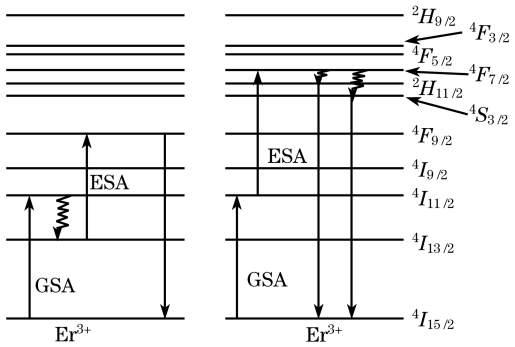

Fig. 4. Schematic diagram for energy levels of Er^{3+} ion in the Y_2O_3 NC and two-photon Up-PL processes under 976-nm excitation. Left: red emission; right: green emission.

excited upconversion luminescence of Er^{3+}-doped Y_2O_3 NC.

The mechanism of the photon avalanche excited upconversion might occur as follows. An Er^{3+} ion is excited to the $^4I_{11/2}$ state by ground state absorption (GSA) of 976-nm photons. Following the excited state absorption (ESA) process, the Er^{3+} ion is further excited to the state $^4F_{7/2}$. By a cross-relaxation process, it then combines with another Er^{3+} ion in the ground state $^4I_{15/2}$ to create two ions in the intermediate state $^4I_{11/2}$. When the pump power exceeds the threshold power, which is 110 mW, cross-relaxation represents the main source of intermediate state population. Both ions can be re-excited to the state $^4F_{7/2}$ again by the laser followed by cross relaxation. In this way, the $^4F_{7/2}$ and $^4I_{11/2}$ populations are gradually build up, thus the term avalanche. Then just like the mechanism discussed above, the Er^{3+} ion in the state $^4F_{7/2}$ decays nonradiatively to the $^2H_{11/2}$ and $^4S_{3/2}$ levels. From these two states, photons in green wavelengths are emitted, and the $^4I_{11/2}$ state ion relaxes nonradiatively to the $^4I_{13/2}$ state, following ESA process, the ion is further excited to the state $^4F_{9/2}$, then the $^4F_{9/2} \rightarrow {}^4I_{15/2}$ red emission occurs. This mechanism is shown in Fig. 5.

When the pump power exceeds 210 mW, as shown in Fig. 3, the slope of the upconversion luminescence intensity versus pump power decreases nonlinearly with the increasing pump power. It should be a "saturation"

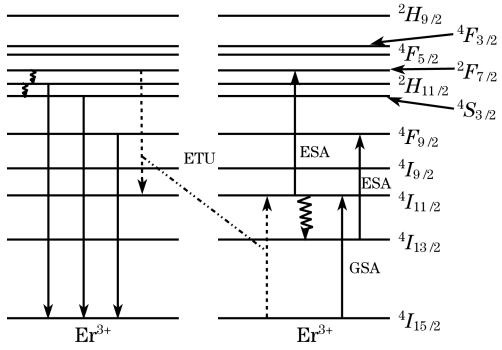

Fig. 5. Schematic diagram for energy levels of Er^{3+} ion in the Y_2O_3 NC and multiphoton Up-PL processes under 976-nm excitation. ETU stands for energy-transfer upconversion. The dashed arrows represent energy-transfer processes.

of the intensity of upconversion luminescence for higher pump powers which was already observed many years ago[14]. Pollnau *et al*. believe that it is determined by the competition between linear decay and upconversion processes for the depletion of the intermediate excited states[12].

In summary, we have investigated the upconversion spectrum and properties of Er^{3+} ions in Er^{3+}-doped Y_2O_3 NCs under 976-nm excitation. We report the photon avalanche upconversion luminescence of Er^{3+} in Er^{3+}-doped Y_2O_3. The green and red emissions originate from two-photon process under low excitation power, and there is a photon avalanche upconversion process under high excitation power (higher than 110 mW). The phenomenon of significantly increased luminescence intensity under high excitation power extends the knowledge of the Er^{3+} ions.

References

1. Z. Wei, L. Sun, C. Liao, C. Yan, and S. Huang, Appl. Phys. Lett. **80,** 1447 (2002).
2. Z. Zhou, T. Komori, T. Ayukawa, H. Yukawa, M. Morinaga, A. Koizumi, and Y. Takeda, Appl. Phys. Lett. **87,** 091109 (2005).
3. A. Patra, C. S. Friend, R. Kapoor, and P. N. Prasad, J. Phys. Chem. B **106,** 1909 (2002).
4. Y. Wu, X. Ma, and X. Zhao, Acta Opt. Sin. (in Chinese) **28,** 1057 (2008).
5. L. Ling, Y. Fu, S. Zhang, and H. Long, Chinese J. Lasers (in Chinese) **35,** 734 (2008).
6. N. Mais, J. P. Reithmaier, A. Forchel, M. Kohls, L. Spanhel, and G. Müller, Appl. Phys. Lett. **75,** 2005 (1999).
7. S. Komuro, T. Katsumata, T. Morikawa, X. Zhao, H. Isshiki, and Y. Aoyagi, J. Appl. Phys. **88,** 7129 (2000).
8. Y. Bai, Y. Wang, K. Yang, X. Zhang, G. Peng, Y. Song, Z. Pan, and C. H. Wang, J. Phys. Chem. C **112,** 12259 (2008).
9. Y. Bai, K. Yang, Y. Wang, X. Zhang, and Y. Song, Opt. Commun. **281,** 2930 (2008).
10. X. Li, Q. Li, J. Wang, and J. Li, J. Lumin. **124,** 351 (2007).
11. C. Wu, W. Qin, G. Qin, D. Zhao, J. Zhang, S. Huang, S. Lü, H. Liu, and H. Lin, Appl. Phys. Lett. **82,** 520 (2003).
12. M. Pollnau, D. R. Gamelin, S. R. Lüthi, H. U. Güdel, and M. P. Hehlen, Phys. Rev. B **61,** 3337 (2000).
13. H.-X. Mai, Y.-W. Zhang, L.-D. Sun, and C.-H. Yan, J. Phys. Chem. C **111,** 13721 (2007).
14. S. Singh and J. E. Geusic, Phys. Rev. Lett. **17,** 865 (1966).